

Visualization of the General Relativistic Rigidly Rotating Disk of Dust

D. Weiskopf¹ and M. Ansorg²

¹Universität Tübingen, Institut für Astronomie und Astrophysik, Auf der Morgenstelle 10,
D-72076 Tübingen, Germany

²Friedrich-Schiller-Universität Jena, Fakultät für Mathematik und Informatik,
Graduiertenkolleg, Ernst-Abbe-Platz 4, D-07743 Jena, Germany
weiskopf@tat.physik.uni-tuebingen.de

Received 29 November 1999, accepted 18 February 2000

Abstract. In this paper the visualization of the rigidly rotating disk of dust is investigated. The visual appearance of the disk as seen by a realistic observer is calculated using the null geodesics of the photons which are emitted by the disk and registered by the observer. This visualization technique is ray tracing in four-dimensional curved spacetime. We create images with a wide range of parameters varying both the position of the observer and the physical properties of the disk in order to obtain interpretations of the basic visual effects. For sufficiently relativistic disks, multiple and distorted images appear. For even more relativistic disks, fractal structures within the image plane occur since neighboring image points correspond to distant points on the disk.

Keywords: general relativity, rigidly rotating disk of dust, visualization, ray tracing

PACS: 04.40.-b, 02.40.-k, 04.25.-g

1 Introduction

In Einstein's general theory of relativity, the geometrical properties of the four-dimensional manifold of space and time are determined by gravitation. As a consequence of the influence of the gravitational field created by a central object (e.g. a black hole or a disk-like formation) on the spacetime structure, the motions of test particles and light rays are considerably affected. Conversely, the study of the paths along which test particles and light rays move conveys information about the underlying geometrical structures.

For the gravitational field created by the rigidly rotating disk of dust, a study of the timelike geodesic motions (i.e. the trajectories of test particles) can be found in [1]. In this paper, we consider large sets of light rays, which follow the null geodesics, in order to give an impression of how the central disk appears to an observer. For creating these images, a visualization technique called ray tracing in four-dimensional curved spacetime is used. It provides a compact presentation of a vast number of light rays and allows for a geometric and intuitive approach. Since the resulting pictures are observables, they are independent of the chosen coordinates in which the metric

is represented. This is an important feature and advantage in the realm of general relativity.

The general relativistic gravitational field created by the rigidly rotating disk of dust was first studied numerically in 1971 by Bardeen and Wagoner[2]. The global analytical solution of Einstein's field equations for this object was found in 1995 by Neugebauer and Meinel[9]. We use their explicit expressions for the metric coefficients in order to create a direct numerical implementation of the geodesic equation. Ray tracing has been used to investigate various objects, e.g. to examine the gravitational effects of a neutron star on null geodesics[11, 7]. A detailed presentation of ray tracing in curved spacetimes can be found in [10].

The paper is organized as follows. First we sketch the structure of the metric tensor and some properties of the rigidly rotating disk of dust. Then we describe the basics of the visualization technique that has been used as well as some details of the numerical implementation. In Sect. 5 we present and discuss the results obtained. We finish with a brief conclusion and some remarks about future intentions.

In what follows, units are used in which the velocity of light as well as Newton's constant of gravitation are equal to 1.

2 The Metric

Einstein's field equations for the rigidly rotating disk of dust can be reduced to a single non-linear complex partial differential equation—the so-called Ernst equation—for which a boundary value problem has to be solved[3, 6]. Neugebauer and Meinel succeeded in solving this problem by means of the inverse scattering method, a technique known from soliton theory.

In Weyl-Papapetrou coordinates (ρ, ζ, ϕ, t) , the metric assumes the form

$$(g_{ij}) = \begin{pmatrix} e^{2(k-U)} & 0 & 0 & 0 \\ 0 & e^{2(k-U)} & 0 & 0 \\ 0 & 0 & -a^2 e^{2U} + \rho^2 e^{-2U} & -a e^{2U} \\ 0 & 0 & -a e^{2U} & -e^{2U} \end{pmatrix}$$

with

$$g_{ij,\phi} = g_{ij,t} = 0,$$

and with g_{ij} possessing reflection symmetry with respect to the plane $\zeta = 0$, i.e.,

$$g_{ij}(\rho, \zeta) = g_{ij}(\rho, -\zeta).$$

The resulting field equations turn out to be equivalent to the Ernst equation

$$\Re f \left(f_{,\rho\rho} + f_{,\zeta\zeta} + \frac{f_{,\rho}}{\rho} \right) = f_{,\rho}^2 + f_{,\zeta}^2$$

for the Ernst potential f which is defined by

$$f = e^{2U} + ib \quad \text{with} \quad b_{,\zeta} = \frac{e^{4U}}{\rho} a_{,\rho}, \quad b_{,\rho} = -\frac{e^{4U}}{\rho} a_{,\zeta}.$$

The remaining metric function k can be calculated from the functions U and a by quadratures.

Neugebauer and Meinel found the Ernst potential for the rigidly rotating disk of dust in terms of ultraelliptic functions[9]. In their expressions, the Ernst potential depends on a parameter μ which is related to the angular velocity Ω and the radius ρ_0 of the disk by

$$\mu = 2\Omega^2 \rho_0^2 e^{-2V_0} \quad \text{with} \quad V_0(\mu) = U(\rho = 0, \zeta = 0; \mu).$$

The parameter μ runs on the interval $(0, \mu_0)$ with $\mu_0 = 4.62966\dots$. For $\mu \ll 1$, the Newtonian limit of the Maclaurin disk is obtained; $\mu \rightarrow \mu_0$ and $\rho_0 \rightarrow 0$ yields the extreme Kerr solution. For $\mu > \mu_e \approx 1.69$, the disk creates a so-called ergoregion within which the metric function ($-e^{2U}$) is positive.

3 Visualization Technique

In this paper, a visualization technique based on ray tracing is used. Normal ray tracing is a computer graphics technique for visualization and photo-realistic rendering. It synthesizes images using a model that inverts the image formation process in nature and that is based on geometric optics. For a detailed presentation we refer to [4].

Rays are traced from the observer through the pixels (picture elements) on the image plane into the scene. The principle is illustrated in Fig. 1. Reflection and refraction rays—secondary rays—are recursively examined when rays intersect objects. Various local illumination models are used in order to compute the light intensity on the object surface at every ray-object intersection point. The specific intensities along a ray contribute to the final intensity and color of the corresponding pixel. The visualization process can be split into two main parts: intersection calculation and local illumination.

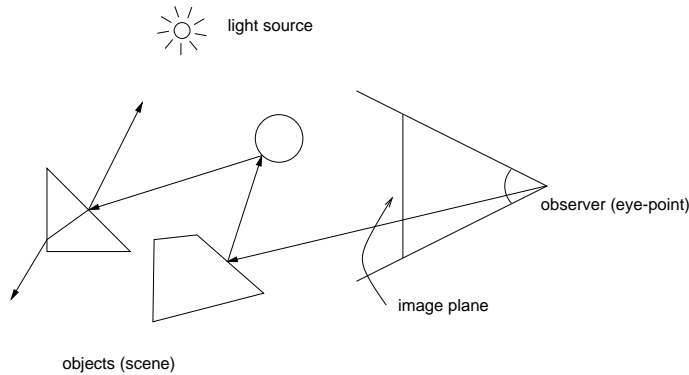


Fig. 1 Ray tracing principle.

In the context of general relativity, two major extensions have to be considered. First, the object space is extended from Euclidean three-dimensional space to four-dimensional spacetime. In general, this curved manifold is described by an atlas. For

the rigidly rotating disk of dust, there exists a single map which completely describes the spacetime in the form of Weyl-Papapetrou coordinates. Therefore, it is sufficient to include an additional time coordinate to the already available spatial coordinates. Secondly, the light rays are no longer straight, but bent rays. These rays are represented by a polygonal approximation with four-dimensional coordinates. This framework automatically takes into account the finite speed of light and its visual effects.

The light rays are identical to null geodesics and can be obtained by solving the geodesic equation

$$\frac{d^2 x^i}{d\lambda^2} + \Gamma_{jk}^i \frac{dx^j}{d\lambda} \frac{dx^k}{d\lambda} = 0, \quad (1)$$

with the null condition

$$g_{jk} \frac{dx^j}{d\lambda} \frac{dx^k}{d\lambda} = 0, \quad (2)$$

where the coordinates x^i describe the location of the points on the light ray, λ is an affine parameter, and Γ_{jk}^i are the Christoffel symbols calculated from the metric tensor. The initial position in spacetime and the initial spatial direction of the light ray are determined by the position, orientation, and field of view of the observer's camera and by the coordinates of the corresponding pixel on the image plane. The time component of the initial direction is fixed by the null condition (2). In this way, the geodesic equation yields an initial value problem for ordinary differential equations. There exist well-known numerical methods for solving this problem, cf., e.g., [12].

In this paper we put emphasis on the investigation of the geometric structure of the null geodesics in the gravitational field of the disk. Therefore, we concentrate on visualizing these properties and we do not intend to generate photo-realistic images. For example, the disk is supposed to be the only light source and its color, intensity, and texture can be freely chosen. In addition, no reflection from or transmission through the surface of the disk is considered. Therefore, recursive examination of secondary rays can be avoided, which reduces computational costs.

4 Implementation

The implementation of the general relativistic ray tracing program is based on the object-oriented and extensible ray tracing system *RayVis*[5], which is written in C++. Extensions are implemented by subclassing relevant parts of the ray tracing system, such as rays, local illumination methods, or geometric objects of the scene. The visualization of the rigidly rotating disk of dust essentially requires two new classes. The first class represents a bent ray in four dimensions and includes a ray generator which uses the Runge-Kutta method[12] to calculate the null geodesics in the gravitational field numerically. The second class represents the rotating disk in four-dimensional spacetime itself, taking into account the motion of the disk.

Due to the vast number of geodesics to be calculated, computation time is an important issue. We address this problem in two ways. First, we accelerate the evaluation of the metric coefficients, which are needed in the form of Christoffel symbols in order

to solve the geodesic equation. The metric coefficients are represented by Chebyshev polynomials and the Chebyshev coefficients are calculated in a preprocessing step. In this way, the time consuming evaluation of integrals and ultraelliptic functions for the metric coefficients can be avoided in the rendering process. Secondly, the ray tracing algorithm is parallelized. Parallelization is based on regions in the image plane, i.e. the rendering of different areas of the image plane is performed by different processors. This is permitted because the calculation of the null geodesics, the intersection points, and the illumination for each pixel is independent of the calculations for the other pixels. The granularity can be adjusted to allow for good load balancing and can be as fine as a single pixel. The implementation is based on MPI (Message Passing Interface)[8]. It is platform independent, it runs on both shared memory and distributed memory architectures, and it scales well on massive-parallel machines such as a CRAY T3E.

5 Results

For a thorough investigation of the null geodesics in the metric of the rigidly rotating disk of dust, we consider a sampling of the parameter space for the null geodesics. The relevant parameters are μ , the position of the observer, and the direction of the incoming light.

The sampling of the direction of the light rays is implemented in the form of a 4π camera, i.e. an observer looking in all directions simultaneously. Here, the projection onto a virtual sphere surrounding the observer is used instead of the projection onto an image plane as described in Sect. 3. Due to time and axial symmetry the t and ϕ coordinates can be neglected. We choose the following values for the remaining parameters:

$$\begin{aligned}\mu &\in \left\{ \frac{n}{4} \mid n \in \mathbb{N}, 1 \leq n \leq 14 \right\}, \\ r/\rho_0 &\in \{0.2, 0.3, 0.6, 1.2, 3, 10\}, \\ \theta &\in \left\{ \frac{n}{10}\pi \mid n \in \mathbb{N}, 0 \leq n \leq 5 \right\},\end{aligned}$$

where $r = \sqrt{\rho^2 + \zeta^2}$ and $\theta = \arctan \zeta/\rho$. The parameter θ can be restricted to the interval $(0, \pi/2)$ because of the reflection symmetry with respect to the plane $\zeta = 0$.

In most cases we use a static camera. In the ergoregion, however, a static observer does not exist. Here, we use a moving observer that is stationary in the frame of reference of the disk.

As a result of the parameter study, we show two typical examples which illustrate the behavior and properties of the null geodesics. Here, the field of view is smaller than 4π and the projection onto an image plane is used again.

The first example is depicted in Fig. 2. Here, the observer is looking at the disk from an outside position which lies in almost flat spacetime. The left image shows a slightly relativistic case with $\mu = 0.7$. The top side of the disk is in light gray, the bottom side is in dark gray. Due to gravitational light bending, both the top and the bottom faces are visible simultaneously. The right image shows a more relativistic situation with $\mu = 3$. Here, multiple images of the top and the bottom emerge. We

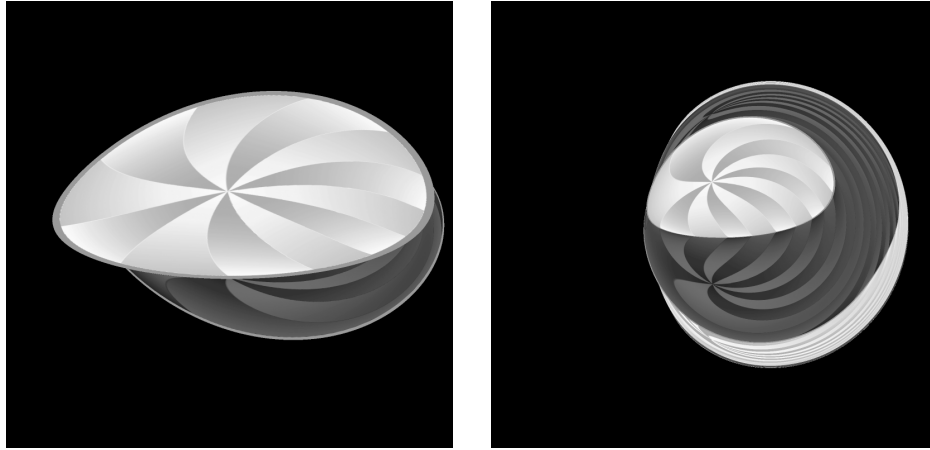


Fig. 2 Visualization of the rigidly rotating disk of dust. In the left image, $\mu = 0.7$ and the observer is located at $\rho = 5\rho_0, \zeta = 1.5\rho_0$. In the right image, $\mu = 3$ and the observer is located at $\rho = 40\rho_0, \zeta = 10\rho_0$.

apply an artificial “pie slice” texture both to the top and the bottom side of the disk in order to visualize rotational distortions. In this way, the effects of frame dragging become clearly visible. (Please note that these are partially occluded by the effects of the finite speed of light and the rotation of the disk.)

The second example is shown in Fig. 3. Here, the position of the observer and the parameter $\mu = 3$ are fixed. The observer is located on the axis of symmetry and looking towards the edge of the disk. The leftmost picture shows a snapshot with a wide angle field of view. Parts of the top side of the disk are visible in the lower part of the picture. An image of the bottom side is found directly above this first image of the top side. Further above, alternating images of the top and the bottom faces follow. The pictures to the right document increasing zooming in on the original picture, whereas the rightmost image shows a part of the leftmost image which has a size approximately ten orders of magnitude smaller than the original image. This series reveals self-similarity and a fractal structure in parts of the ray-traced images.

Further images and movies containing results of the visualization of the rigidly rotating disk of dust can be found on our project web site[13].

6 Conclusion and Future Work

We have investigated the spacetime properties of the rigidly rotating disk of dust by using four-dimensional ray tracing as a means of visualization. The visualization shows typical effects of a strong gravitational source, such as bending of light rays and multiple images of the same object. Frame dragging induced by the rotation of the disk is clearly visible. In addition, a fractal structure and self-similarity emerge in some areas of the ray-traced images.

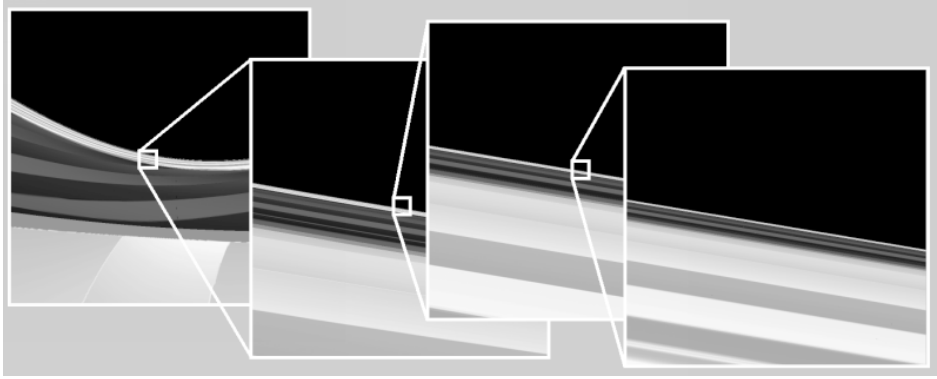


Fig. 3 Fractal structures and self-similarity. The observer is located on the symmetry axis with $\zeta = \rho_0$ and is zooming in on the image. The parameter $\mu = 3$.

In future work, we will investigate the fractal properties in more detail. Furthermore, background objects will be considered in order to examine gravitational lensing beyond the position of the disk. Finally, we will include effects on the apparent color and brightness induced by the gravitational red shift, the Doppler effect, and the transformation of specific intensity.

This work was supported by the Deutsche Forschungsgemeinschaft (DFG) and is part of the project D4 within the Sonderforschungsbereich 382. We would like to thank W. Schweizer and the participants of the Journées Relativistes '99 for fruitful remarks and discussions, in particular A. Kleinwächter, R. Meinel, G. Neugebauer, J. Podolský, and H. Ruder. Thanks to D. Petroff and B. Salzer for proof-reading.

References

- [1] M. Ansorg, *J. Math. Phys.*, **39** (1998) 5984
- [2] J. M. Bardeen and R. V. Wagoner, *Astrophys. J.* **167** (1971) 359
- [3] F. J. Ernst, *Phys. Rev.*, **167** (1968) 1175
- [4] A. S. Glassner, editor, *An Introduction to Ray Tracing*, Academic Press, 1989
- [5] A. Gröne, *Entwurf eines objektorientierten Visualisierungssystems auf der Basis von Raytracing*, PhD thesis, University of Tübingen, 1996
- [6] D. Kramer and G. Neugebauer, *Commun. Math. Phys.* **7** (1968) 173
- [7] U. Kraus, in *Relativistic Astrophysics* edited by H. Riffert, H. Ruder, H.-P. Nollert, and F. W. Hehl, Vieweg, 1998, pp. 66–81
- [8] *Message Passing Interface Forum*, Web Site: <http://www.mpi-forum.org>
- [9] G. Neugebauer and R. Meinel, *Phys. Rev. Lett.* **75** (1995) 3046
- [10] H.-P. Nollert, U. Kraus, and H. Ruder, in *Relativity and Scientific Computing* edited by F. W. Hehl, R. A. Puntigam, and H. Ruder, Springer, 1996, pp. 314–329
- [11] H.-P. Nollert, H. Ruder, H. Herold, and U. Kraus., *Astron. Astrophys.* **208** (1989) 153
- [12] W. H. Press, S. A. Teukolsky, W. T. Vetterling, and B. P. Flannery, *Numerical Recipes in C*, Cambridge University Press, second edition, 1994
- [13] D. Weiskopf, *SFB 382 – Project D4*, Web Site: <http://www.tat.physik.uni-tuebingen.de/~weiskopf>